# Monitoring of a preseismic phase from its electromagnetic precursors

Y. F. Contoyiannis,[1,*] P. G. Kapiris,[2,†] and K. A. Eftaxias[2,‡]
[1]*Technological Educational Institute of Chalkis, Chalkis, Greece*
[2]*Solid State Section, Physics Department, University of Athens, Athens, Greece*
(Received 22 March 2004; revised manuscript received 31 August 2004; published 22 June 2005)

Fracture in disordered media is a complex problem for which a definitive physical and theoretical treatment is still lacking. We view earthquakes (EQ's) as large-scale fracture phenomena in the Earth's heterogeneous crust. Our main observational tool is the monitoring of the microfractures, which occur in the prefocal area before the final breakup, by recording their kHz–MHz electromagnetic (EM) emissions, with the MHz radiation appearing earlier than the kHz. Two fundamental questions (unanswered yet) that scientists in this field ought to address are as follows. (i) Is there a way of estimating the time to global failure? (ii) Is the evolution towards global failure irreversible after the appearance of distinguishing features in the preseismic EM time series? We attempt to put forward physically powerful arguments with regard to answering these two basic questions. Our approach will be in terms of critical phase transitions in statistical physics, drawing on recently published results. We obtain two major results. First, the initial MHz part of the preseismic emission, which has antipersistent behavior, is triggered by microfractures in the highly disordered system that surrounds the essentially homogeneous "backbone asperities" within the prefocal area and could be described in analogy with a thermal continuous phase transition. However, the analysis reveals that the system is gradually driven out of equilibrium. Considerations of the symmetry-breaking and "intermittent dynamics of critical fluctuations" method [1] estimate the time beyond which the process generating the preseismic EM emission could continue only as a nonequilibrium instability. Second, the abrupt emergence of strong kHz emission in the tail of the precursory radiation, showing strong persistent behavior, is thought to be due to the fracture of the high-strength "backbones." The associated phase of the EQ nucleation is a nonequilibrium process without any footprint of an equilibrium thermal phase transition. The family of asperities sustains the system. Physically, the appearance of persistent properties may indicate that the process acquires a self-regulating character and to a great degree the property of irreversibility, one of the important components of predictive capability. We address the role of the order of material heterogeneity on the transition from antipersistent to persistent behavior.

DOI: 10.1103/PhysRevE.71.066123 PACS number(s): 64.60.Ht, 62.20.Mk, 64.60.Ak, 91.30.Px

## I. INTRODUCTION

Fracture in disordered media is a complex problem for which a definitive physical and theoretical treatment is still lacking. Earthquakes (EQ's) are large-scale fracture phenomena in the Earth's heterogeneous crust. A vital problem in material science and in geophysics is the identification of precursors of macroscopic defects or shocks. Here we shall focus on the geophysical view of this problem, but will also discuss relevant laboratory observations.

Crack propagation is the basic mechanism of materials failure. When a heterogeneous material is strained, its evolution toward fracture is characterized by local nucleation and coalescence of microcracks before global failure. Both acoustic and electromagnetic (EM) emissions in a wide frequency spectrum ranging from very low frequencies (VLF's) to very high frequencies (VHF's) are produced by the opening of microcracks. These emissions are considered as precursors of general fracture. These precursory phenomena are detectable both on a laboratory and on a geophysical scale. A recent analysis by Kapiris *et al.* [1] in terms of prefracture EM emission reveals that the same critical fractoelectrodynamics may hold from the geophysical scale down to the microscopic scale of the sample's rheological structure. In addition, these authors observe a striking accord of critical exponents between acoustic emission and EM emission induced by rock fracture, which further supports the hypothesis that the opening crack emits both acoustic and EM pulses.

Our main observational tool is the monitoring of the microfractures, which occur in the prefocal area before the final breakup, by recording their VLF (kHz) to VHF (MHz) EM emissions. Clear VHF-to-VLF EM anomalies have been detected over periods ranging from a few days to a few hours prior to recent destructive EQ's in Greece, with the VHF radiation appearing earlier than the VLF [2]. In principle, it is difficult to establish a particularly strong connection between two events that are separated in a time span such as that between a preseismic EM emission and the impending event. Because of this, we have attempted in recent work a multidisciplinary study of the recorded field anomalies [1–9]. The study supports the association of the recorded EM anomalies with the fracture process in the prefocal area.

The purpose of this paper is to study two fundamental questions that are as yet unanswered. (i) Is there a way of estimating the time to global failure? (ii) Is the evolution towards global failure irreversible after the appearance of

*Electronic address: ycont@panafonet.gr
†Electronic address: pkapiris@cc.uoa.gr
‡Electronic address: ceftax@phys.uoa.gr

 

distinguishing features in the prefracture EM time series? Here we attempt to put forward physically powerful arguments which may shed light on these two questions.

In the remainder of this section we briefly present the structure of our work. In Sec. II we report on the connection between EM signals and microfracturing activity.

In Sec. III we introduce the essential concepts of the intermittent dynamics of critical fluctuation (IDCF) method [10,11]. This method has shown that fluctuations in the order parameter, corresponding to successive configurations of a critical system in thermal equilibrium, obey a dynamical law of type-I intermittency.

Our model of the focal area consists of (i) a backbone of strong and almost homogeneous large asperities that sustains the system and (ii) a strongly heterogeneous medium that surrounds the family of strong asperities. We distinguish two characteristic epochs in the evolution of precursory EM activity and identify them with the equivalent critical stages in the EQ preparation process.

The first epoch includes the initial VHF (MHz) antipersistent part of the precursory EM emission. In Secs. IV–VII we establish the hypothesis that the VHF precursory EM emission originates during microcracking in the highly heterogeneous component. There, weaker areas and smaller asperities can rupture earlier than stronger areas and larger asperities, and thus the rupture is finally obstructed at the boundary of the backbone of strong asperities.

Growing evidence suggests that rupture in strongly disordered systems can be viewed as a type of critical phenomenon—e.g., [12–16]. The application of the IDCF method (Sec. IV) verifies that the source of the initial VHF phase of the precursory EM activity can be described as analogous to a second-order phase transition: from the phase of a sparse almost symmetrical random cracking distribution to a localized cracking zone that includes the backbone of strong asperities.

A characteristic signature of the onset of a continuous (second-order) phase transition is symmetry breaking (SB). This signature is hidden in the VHF preseismic time series (Sec. V). The SB here lies in the transition from nondirectional uncorrelated to directional correlated crack growth. This finding further supports the hypothesis that the rupture in disordered systems can be viewed as a type of critical phenomenon.

Recent statistical fractal spectral analysis [3] reveals that changes with time of the associated scaling dynamical parameters emerge as the main shock is approached. These changes reveal that the system is gradually driven out of equilibrium. Thus, we try to determine up to what time the preseismic EM phenomenon shows footprints of a classical equilibrium phase transition. In Sec. V we study this subject in terms of "symmetry breaking." We are interested not only in the appearance of the latter but also in its temporal evolution.

We attempt in Secs. VI and VII to establish a connection between the characteristic critical $p_l$ exponent associated with the IDCF method and the Hurst exponent, which describes the antipersistente and persistent behavior of the EM time series. The $H$ exponent is determined in consecutive time intervals of small duration. It is implied by the IDCF method that the allowed range of $p_l$ values for a second-order phase transition is $p_l > 1$. The connection between $p_l$ and $H$ leads to the suggestion that the maximum allowable value of $H$ for a second-order phase transition is 0.5. This is a crucial value characterizing the transition of a system from antipersistent $(0 < H < 0.5)$ to persistent $(0.5 < H < 1)$ behavior. Consequently, we suggest that rupture in the focal area can be described in terms of a second-order phase transition until the moment that the preseismic time series shows persistent behaviour—i.e., until the local Hurst exponent exceeds 0.5. The analysis reveals an increase with time of $H$ exponent in the VHF EM time series, but within the range (0, 0.5). We argue that the interplay between the heterogeneities in the prefocal area and the stress field could be responsible for the observed antipersistent pattern of the precursory VHF EM time series. Interestingly, the SB is completed when the $H$ exponent is shifted close to 0.5, and it happens in the tail of the VHF EM radiation. This observation (i) confirms the result using the IDCF method that the interval $0 < H < 0.5$ implies an underlying second-order phase transition in equilibrium and (ii) may indicate that the "siege" of the backbone of strong asperities, which sustains the system, has already been started. Microcracking will then occur in the strong asperities if the local stress exceeds fracture stress.

The second characteristic epoch in the evolution of precursory EM activity includes the last stage of the precursory VLF EM radiation. In Sec. VII we emphasize that it is mainly characterized by strong multipeaked signals with both sharp onsets and falloffs that show persistent behavior; namely, the associated Hurst exponent $H$ varies from 0.5 to 1. *This final part of the radiation evolves as a phase transition far from equilibrium without any footprint of an equilibrium phase transition*. The presence of persistent properties in the tail of the precursory EM phenomenon indicates that the fracture acquires the property of irreversibility. We suggest that this radiation is due to the fracture of the high-strength large asperities. In Sec. VIII we present further evidence indicating the fracture of asperities.

In Sec. IX we discuss the EM quiescence observed in all frequency bands just before global failure. The main results of the present work are summarized in Sec. X.

We stress that in order to study a preseismic EM phenomenon based on concepts of statistical physics it must satisfy the following requirements. (i) It must have a long duration in order to include information associated with the last stages of the EQ preparation process. Additionally, a long duration is required for its statistical analysis. (ii) It must have been recorded in various narrow frequency bands, distributed in the kHz–MHz range. This is consistent with field and laboratory experience, according to which the main part of the emission spectrum is significantly shifted from higher- to lower-frequency bands as the global failure is approached. (iii) The recorded radiation must be very clear and representative of the fracture process, which means it has not been significantly absorbed by the conducting crust. This implies that the EM precursor must be associated with an in-land seismic event which is both strong and shallow.

Over a period of ten years of experimental work, only two of the collected preseismic EM signals satisfy all the aforementioned criteria. These two are associated with the

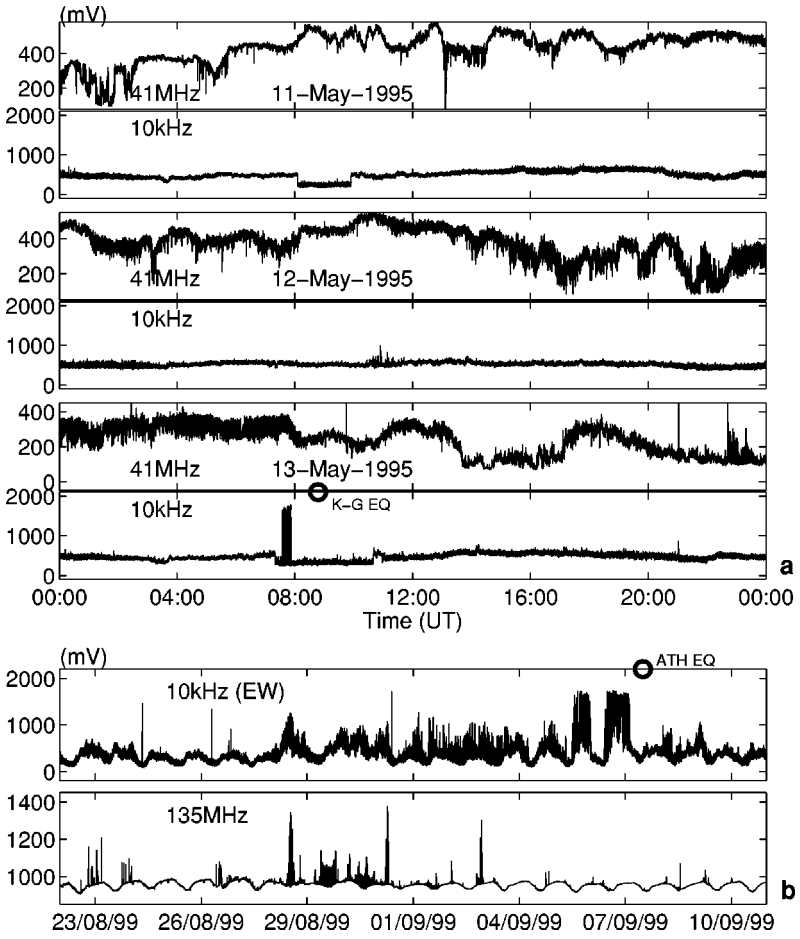


FIG. 1. (a) Electromagnetic anomalies detected before the $M=6.6$ Kozani-Grevena earthquake on 13 May 1995 at 08:47:12,9 (UTC) at 41 MHz and 10 kHz. We observe an almost simultaneous cessation of these EM signals at both (kHz and MHz) frequency bands almost 1 h before the earthquake although they hand different onsets times. (b) Electromagnetic anomalies detected prior to the $M=5.9$ Athens earthquake occurred on 7 September 1999 at 11:56 UTC at 135 MHz and 10 kHz. The electromagnetic anomalies ceased almost 9 h before the earthquake.

Kozani-Grevena (KG) EQ and the Athens EQ (see Fig. 1). In order to further validate our results based on these EQ's, we have systematically investigated whether the results of the present analysis are in agreement with laboratory findings on fracture in rocks.

## II. EM RADIATION ACCOMPANYING FRACTURES IN SOLID MATERIALS

Prefracture EM radiation is a multiscale phenomenon that is currently under investigation in the field (before EQ's) and in the laboratory. It has been detected during fracture in various materials, including metals, alloys, single crystals, rocks, and ice [17–27]. In addition, sufficient experimental results illustrating the connection between anomalous VLF-VHF EM phenomena and EQ preparation have been presented in a rather comprehensive collection of papers [28–31].

Laboratory evidence indicates that EM and acoustic emissions are two sides of the same coin, both caused by crack formation and growth ("laboratory earthquakes"). This statement is supported by the following. (i) The onset time of EM emission was found to coincide with that of acoustic emission [20,27,32–34]. (ii) Simultaneous EM and acoustic pulses associated with the same microcracking event have been recorded in both piezoelectric material and nonpiezoelectric ionic crystals [27]. (iii) Various authors [26,35] have accurately measured and parametrized individual pulses of EM radiation during a fracture experiment and correlated them with crack dimensions directly.

Several atomic models have been put forth to explain the origin of EM emission (e.g., [26] and references therein) [28–31]. Consider in particular the "movement of charged crack surfaces." In this model, when a crack opens the rupture of interatomic (ionic) bonds leads to intense charge separation [36–38]. Direct evidence of a surface charge of opposite polarity on fresh fracture surfaces has been provided by Wolibrandt *et al.* [39]. Simultaneous measurements of the electron, ion, and photon emission (fractoemission) accompanying fracture support the hypothesis that charge separation accompanies the formation of fracture surfaces [36,40–42]. On the faces of a newly created crack the electric charges constitute an electric dipole (or a multipole of higher order), and due to crack wall motion, EM radiation is emitted [32,34]. Experiments performed by Kuksenko [43] for several materials such as glass, alkali-halide crystals, and several rock specimens support this hypothesis. Additional evidence for this mechanism was provided by Khatiashvili [44], who investigated the spectral features of prefracture EM emission, and by O'Keefe and Thiel [45], who studied the phenomenon during ice compression. Crack motion in fracture dynamics has recently been shown to be governed by a dynamical instability, which causes oscillations in the crack velocity and structure on the fracture surface. Evidence indicates that the instability mechanism is local branching; i.e., a multicrack state is formed by repetitive, frustrated mi-

crofracturing events [46–48]. Local branching obeys a power law which may provide an explanation for the scaling behavior of fracture surfaces that has been observed in many materials [49]. Laboratory experiments show intense EM fractoemission during this unstable crack growth [41]. In this unstable stage we regard the emission from the correlated population of fractoemissions as a precursor of the final global instability.

We recently introduced a model for the generation of preseismic EM emissions which explains the observed phenomenology in terms of microcrack geometry and fractal electrodynamics [8]. The EQ's occur on a fractal structure of faults [1,50]. We consider that the emitting, diffusing, and recombination charge accompanying the microfracture acts as a current. From this point of view an active crack or rupture can be regarded as a "radiating element." The idea is that as the critical point is approached, an array of line elements having a fractal distribution on the ground can form a fractal geoantenna. We have tested this idea in terms of fractal electrodynamics, which combines fractal geometry with Maxwell's equations of electrodynamics [51,52].

We cite the following experimental evidence. A clear VLF EM emission was recorded during the last few days before the Athens EQ [see Fig. 1(b)]. The statistical analysis reveals that the cumulative number $N(>A)$ of EM events—namely, the number of EM events having amplitude larger than $A$—follows the power law [1] $N(>A) \sim A^{-0.62}$. Rabinovitch *et al.* [25] have studied the fractal nature of EM radiation induced in rock fracture. The analysis of the prefracture EM time series reveals that the cumulative distribution of the amplitudes also follows a power law with exponent 0.62. The accord of the critical exponents suggests that the same fractoelectrodynamics may hold from the geophysical down to the microscopic scale [1]. In addition, scaling similarities of acoustic and EM emissions during multiple fracture in solid materials from the laboratory scale up to the geophysical scale strongly support the hypothesis that both types of emission are generated during crack opening [1].

## III. INTERMITTENT DYNAMICS OF CRITICAL FLUCTUATION METHOD

In a recent paper [10] we propose a statistical method of analysis for the critical fluctuations in systems which undergo a continuous phase transition at equilibrium. This method is based on a previous work of ours, according to which the fluctuations of the order parameter at the critical point of a continuous phase transition obey an intermittent dynamics which can be analytically expressed by a one-dimensional map of intermittency type I [11]. The IDCF method has been applied in numerical systems such as the three-dimensional (3D) Ising model [10], as well as in nonthermal real systems such as preseismic fractures [9] and biological systems [53].

In what follows we give an overview of the IDCF method. We refer the reader who is interested in more theoretical details to [10,11].

The exact dynamics at the critical point can be analytically determined for a large class of critical systems by the so-called critical map (CM). For small values of the order parameter $\phi$ this map can be written

$$\phi_{n+1} = \phi_n + u\phi_n^z + \epsilon_n, \tag{1}$$

where $\phi_n$ is defined as $\phi_n = |\bar{\psi} - \psi_n| / \Delta\psi$. Here $\bar{\psi}$ is the marginally unstable fixed point and $\Delta\psi$ the suitable range of values $\psi$ ensuring $0 \leqslant \phi < 1$. The exponent $z$ is related to the isothermal critical exponent $\delta$ as $z = \delta + 1$. The shift parameter $\epsilon$ introduces a stochastic noise.

The exact solution for the CM possesses, apart from the extended laminar region near the values $\phi \approx 0$, a superexponential decreasing region, which acts as a kick mechanism for a given trajectory leading it through one iteration back to the laminar region (see Fig. 1 in Ref. [11]).

The invariant density $\rho(\phi)$ of such a map is characterized by a plateau which decays in a superexponential way (Fig. 2 in Ref. [11]).

The first part of the CM follows the bisector, like the tent map, in the limit where the slope tends to 1. It is known [54] that in this limit the Liapunov exponent of the tent map tends to zero and the corresponding trajectories possess a laminar behavior. It is also known that the invariant measure of the tent map is a uniform function. Therefore we conclude that the plateau region of the invariant density $\rho(\phi)$ corresponds to the laminar region of the CM, where fully correlated dynamics takes place. But due to the fact that the dynamical law (1) changes continuously with $\phi$, the end of the laminar region is not strictly defined and therefore should be treated as a varying parameter.

The distribution of the laminar intervals in the limit where $\epsilon_n \to 0$ is given by the power law [54]

$$P(l) \sim l^{-p_l}, \tag{2}$$

where the exponent $p_l$ is connected with the exponent $z$ by

$$p_l = 1 + \frac{1}{z-1}. \tag{3}$$

Inversely, the existence of a power law such as Eq. (2) is a signature of an underlying correlated dynamics associated with the critical behavior. Indeed, it is straightforward to show that if the time series is dominated by a random process, then the corresponding distribution of the lengths of the laminar region should be exponential. In fact, in this case, if the probability of being in the plateau region is $q$, then the corresponding distribution $\tilde{P}(l)$ should be

$$\tilde{P}(l) = ce^{-l\ln(1/q)}, \quad c = \text{const}.$$

The universal character of critical phenomena gives meaning to the exponent $p_l \equiv 1 + 1/(z-1)$ beyond a thermal phase transition. By definition the exponent $p_l > 1$ because in critical phenomena we have $\delta > 0 (z > 1)$.

We present now a process for investigating criticality in a nonequilibrium system.

We proceed by searching windows in a time series, where the distribution of their values $\psi$ is similar in form to the CM invariant density; namely, it demonstrates a plateau which decays in a characteristic way—e.g., exponential or abrupt.

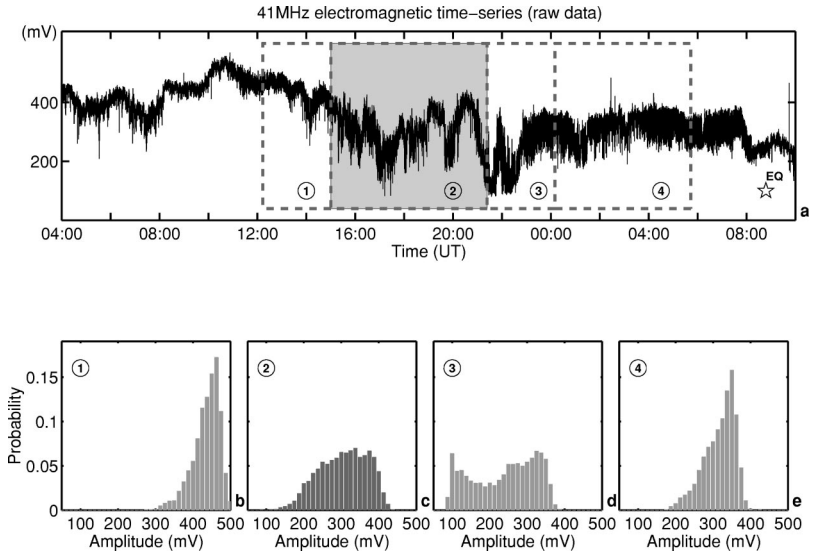


FIG. 2. (a) shows the 41-MHz time series associated with the Kozani-Grevena earthquake. The star indicates the time of the earthquake occurrence. (b)–(e) show the distribution of the amplitude of electromagnetic pulses for four consecutive time intervals marked in (a). The second (shaded) time interval determines, in terms of the IDCF method [10], the crucial time interval during which the short-range correlations evolve to long range (critical window); the corresponding distribution (c) might be considered to be a precursor of the impending symmetry breaking readily observable in the subsequent time interval (d). The distribution in (e) is very similar to that of (b), while here there is an upward shift of the values to the range of the second lobe of the distribution in (d); the appearance of the distribution in the (e) may indicate that the symmetry breaking in the underlying fractoelectromagnetic mechanism has been almost completed. The aforementioned evolution is expected in the framework of the hypothesis that the fracture in the highly disordered media develops as a kind of generalized continuous phase transition.

A cumulative stationary condition is necessary for the application of the IDCF method to nonequilibrium systems. The search for stationary behavior is done inside the time series windows.

We look for a nontrivial dynamics within the windows. This is accomplished as follows.

We produce the distribution $P(l)$, where the $l$ is the laminar interval—namely, the stay time within the laminar region. The $k$th laminar interval $l_k$ is determined by counting the number of successive values $\psi_l$ of EM fluctuations fulfilling the condition $\psi_l \leqslant \psi_i \leqslant \psi_o$, $i=k+1,\ldots,k+l$, where $\psi_o$, $\psi_l$ are the bounds of the laminar region. The value of $\psi_o$ is essentially the origin of the plateau. The end of the laminar region $\psi_l$ is put in the decay region and, as mentioned previously, will be treated as a parameter. Using the fitting function $P(l)=p_1 l^{-p_2} e^{-p_3 l}$ we estimate the exponents $p_2, p_3$ for different values of $\psi_l$. Each pair $(p_2, p_3)$ characterizes a sequence of values (a trajectory) which corresponds to the laminar region $[\psi_0, \psi_l]$. Generally, small values for the exponent $p_3$ (near 0) and $p_2$ values greater than 1 indicate that the time series possesses an intermittent component similar to the dynamics of the fluctuations of the order parameter in a critical thermal system. In the ideal case, for a data set with very high statistics, the $p_2$ values are almost equal to each other and the $p_3$ exponents are very close to 0. For these cases the critical exponent $p_l$ is the common (or mean) value of $p_2$.

In the next sections, we apply the IDCF method to the initial VHF component of the recorded preseismic EM activities prior to the KG EQ.

## IV. APPLICATION OF THE ICDF METHOD TO THE DETECTED PRESEISMIC VHF RADIATION

We refer to the preseismic 41-MHz EM signal detected prior to the KG EQ [Fig. 1(a)]. The data are sampled at 1 Hz. We find a window including 23 000 points, starting almost 11 h before the time of the EQ, in which a cumulative stationary condition occurs. As mentioned above, cumulative stationary behavior in the time series is a necessary condition for applying the IDCF method to a nonequilibrium process. We shall refer to the corresponding window as a "critical window" (CW). The stationary behavior of the CW can be checked by estimating the mean value and the standard deviation for various time intervals in the CW, all having a common time origin. The results are shown in Fig. (2a) of Ref. [9]. (In Sec. V, where we analyze the second example of preseismic signals associated with the Athens EQ, we will demonstrate in detail how the cumulative stationary estimation is done.) In our Fig. 2(a), the signal of EM fluctuations in the 41-MHz channel is shown. We have identified four characteristic time intervals in this signal, and the corresponding distributions of the amplitude of the EM pulses are shown in Figs. 2(b)–2(e). All these windows include the maximum number of experimental points before the distribution begins to change form.

The distribution in Fig. 2(c) is of the form indicating a CW. It shows the characteristics of an invariant density of a CM—namely, a plateau (with some fluctuations) and the decay on the left.

The next step in the analysis is to produce the distribution $P(l)$ where the length $l$ is the laminar interval—i.e., the stay

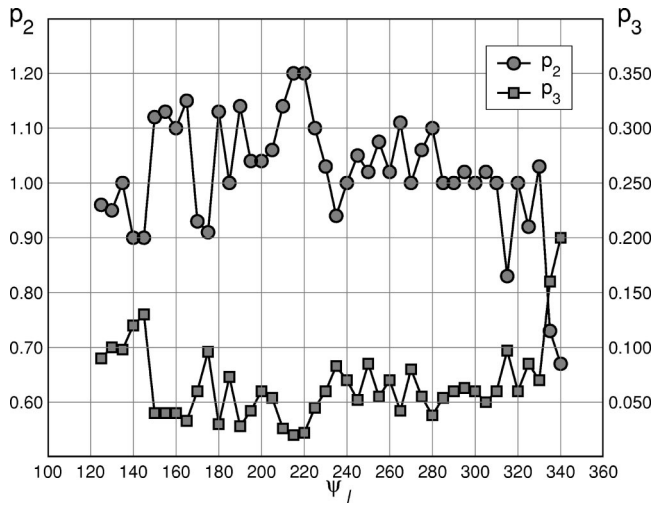


FIG. 3. The exponents $p_2$, $p_3$ versus the end of laminar region $\psi_l$. The analysis refers to the KG EQ case.

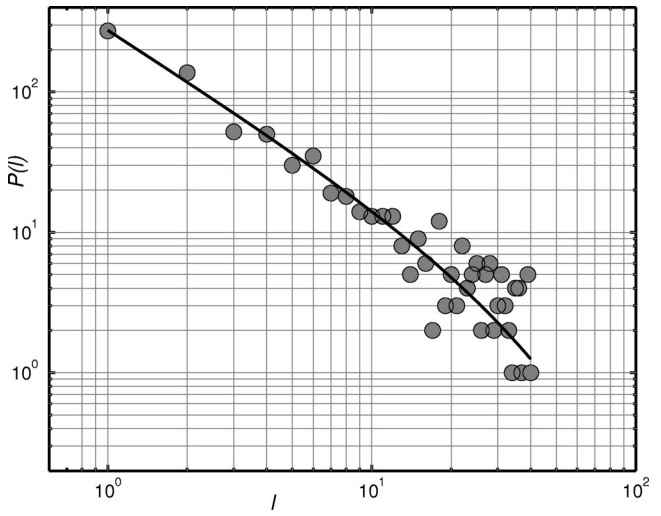


FIG. 4. The distribution $P(l)$ of the laminar intervals $l$. The solid line represent the fitting function $P(l)=p_1 l^{-p_2} e^{-p_3 l}$. The analysis refers to the KG EQ case.

time within the laminar region. The $k$th laminar interval $l_k$ is determined by counting the number of succesive $\psi_i$ values of EM signal fulfilling the condition $\psi_l \leqslant \psi_i \leqslant \psi_o$, $i=k+1,\ldots,k+l$, where $\psi_o$, $\psi_l$ are the bounds of the laminar region. The value of $\psi_o$ is essentially the origin of the plateau (corresponding to the marginally unstable fixed point $\bar{\psi}$, which here has the value $\approx 387$). We treat the end of the laminar region $\psi_l$ as a variable parameter inside the decay region. Using the fitting function $P(l)=p_1 l^{-p_2} e^{-p_3 l}$ we estimate the exponents $p_2, p_3$ for different values of $\psi_l$ as shown in Fig. 3.

In Fig. 3 we see that almost all trajectories have small exponents $p_3$ and the corresponding exponents $p_2$ have values equal to or greater than 1. Therefore almost all the trajectories have an intermittent character similar to thermal critical systems. It is also clear that where the $p_3$ becomes a minimum the exponent $p_2$ becomes a maximum. From Fig. 3 these extremes are $p_3=0.022\pm0.003$ and $p_2=1.20\pm0.01$. For these values the distribution $P(l)$ (Fig. 4) is closest to the power law (2) and therefore the corresponding exponent $p_2$ is closest to the critical exponent $p_l$.

The above analysis indicates that during the CW the fluctuations of the amplitude $\psi_i$ of the recorded preseismic EM time series have an intermittent behavior similar to the dynamics of the order parameter's fluctuations of a thermal critical system at the critical temperature. It is for this reason that we refer to this time interval as a "critical window." This finding indicates the critical character of the underlying fracture mechanism characterized by the presence of long-range correlations as well as fluctuations at many different time scales.

## V. SYMMETRY-BREAKING PHENOMENON

A thermal second-order phase transition is associated with a "symmetry breaking." To gain insight into the catastrophic character of fracture phenomena, we will elucidate the evolution of the SB with time for the nonequilibrium, irreversible process discussed here by making an analogy to a thermal continuous phase transition. In the latter, the distribution of the fluctuations of the order parameter with temperature reveals the progress of the SB. This distribution is almost a $\delta$ function at high temperature and evolves to a Gaussian with mean value zero as the system approaches the critical point. At the CP a characteristic plateau in the distribution appears, and the SB emerges as the temperature further decreases [10]. Below the critical temperature the distribution becomes again Gaussian but its mean shifts to higher values associated with the SB. As $T$ approaches 0 K, where the SB is completed, it becomes a $\delta$ function again. We look for these characteristic features in the preseismic time series, with stress taking on the role of temperature.

### A. Order parameter

The question of whether rupture exhibits the properties of a first-order or a second-order phase transition remains under discussion, as well as the nature of the order parameter that indicates the type of transition [55]. As mentioned, during the CW the fluctuations of the amplitude $\psi_i$ of the preseismic EM time series have an intermittent behavior similar to the dynamics of the order parameter's fluctuations of a thermal critical system at the critical temperature. This implies that the amplitude $\psi_i$ behaves as a kind of order parameter.

In a recent Letter, Moreno *et al.* [55] explored through numerical simulation the criticality of fracture in heterogeneous materials. Following [56], Caldarelli *et al.* [57] introduce the branching ratio $\zeta$ for each avalanche. This parameter represents the probability of triggering future breaking events given an initial individual failure and is related to the number of broken bonds by

$$\zeta = \frac{\langle z \rangle - 1}{\langle z \rangle}, \tag{4}$$

where $\langle z \rangle$ represents the average number of elements that fail in one avalanche, which is a function of the control param-

eter $\sigma$ (stress). The above relation can be obtained by thinking of the evolution of fracture as a branching process [58]. In this process, each node gives rise to a number $n$ of new branches in the next time step. The average number of $\langle n \rangle$ is called the branching ratio $\zeta$. The branching ratio takes the value 1 when the system is critical, so its value at any prior time represents a measure of how close the system is to criticality. The branching ratio then acts as an *order parameter*.

Interestingly, due to the behavior of the branching ratio, it has been suggested that fracture in heterogeneous systems with long-range interaction can be described as analogous to a second-order phase transition [59].

As mentioned in Sec. II, the intensity of the prefracture EM emission gives a measure of the rate of broken bonds. The preseismic EM time series was sampled at 1 Hz. Thus, the amplitudes $\psi_i$ of the recorded EM time series constitute a measure of $\zeta$, the number $\langle n \rangle$ of bonds broken in the time interval from $t_{i-1}$ to $t_i$. In the language of phase transitions, we consider the amplitude $\psi_i$ of the intensity of the recorded EM radiation as proportioned to the order parameter.

The control parameter can be taken as the stress [59] or the time, if we suppose that the stress increases linearly with time.

### B. Symmetry breaking in the case of the KG EQ

Let us look specifically at the preseismic VHF EM anomaly associated with the KG EQ. Figures 2(b)–2(e) exhibit the distribution of the recorded EM fluctuations in successive time windows. As mentioned the distribution of the amplitude $\psi_i$ of the preseismic EM time series in Fig. 2(c) is of the form indicating a CW. The distributions of the fluctuations of the order parameter in Figs. 2(b) and 2(c) in Ref. [10] reveal the SB in a thermal-critical system (3D Ising model). A simple comparison between these figures and our Figs. 2(c) and 2(d) indicates clearly the similarity between the corresponding distributions. We note that the distribution in Fig. 2(d), which indicates the emergence of SB, separates into two characteristic lobes. Let us focus on Figs. 2(b) and 2(e). Figure 2(b) shows the distribution before the emergence of the "critical window." This distribution may be considered as a precursor of the impending critical window. Figure 2(e) shows the distribution after the beginning of SB. This distribution is very similar to that of Fig. 2(b). However, here there is an upward shift of the values to the range of the second lobe of the distribution in Fig. 2(d). The appearance of the distribution in Fig. 2(e) may indicate that the SB in the underlying fracto-EM mechanism has been almost completed.

It is generally accepted that the terminal phase of the EQ preparation process is accompanied by a significant increase in localization and directionality. The completion of the SB may signal that microfractures in the heterogeneous component of the prefocal area, which surrounds the backbone of strong asperities on the fault plane, have finished: the "siege" of the backbone of asperities begins. Note that the SB is complete $\sim$3 h before the cessation of the EM precursor.

*We think that the second-order phase transition analogy of the EQ preparation process can be carried only up to this point*.

### C. Physical background behind the evolution of the symmetry breaking

Theoretical studies as well as experimental observations from the geophysical scale up to laboratory scale verify that microcracks, isolated in space and time, emerge during the initial stages of the fracture process in heterogeneous media. These subsequently grow and multiply. This leads eventually to cooperative effects associated with the appearance of a clearly preferred direction of elementary fracture activities just before the global failure. So the symmetry in the spatial distribution of opening cracks is broken. We suggest that the observed "symmetry breaking" is the transition from a sparse almost symmetrical random cracking to a localized cracking zone that includes the backbone of strong asperities. This is analogous to the transition from a paramagnetic to a ferromagnetic system, where symmetry is broken because of a spontaneous magnetization that defines a unique direction in space. The following theoretical and experimental information supports this suggestion.

Kolesnikov and Chelidze [60] have introduced the model of anisotropically correlated percolation. The major points of this model are that (i) elementary ruptures interact due to overlapping of their (scalar) stress field, giving rise to correlation effects, and (ii) at the same time the action of anisotropy inherent in the material leads to the existence of preferred directions in the arrangement of elementary ruptures. Thus both correlation and anisotropy should be taken into account simultaneously [61]. Both properties are hidden in the pre-seismic EM time series.

The fractal analysis of the VHF preseismic EM emission associated with the KG EQ verifies that the underlying fracture process evolves under the constraint of increasing in the spatially anisotropic distribution of fracture events. Indeed, the appearance of a preferential direction should undoubtedly reduce both the multifractality and the fractal dimension. We cite the following evidence.

(i) Following Ivanov *et al.* [62] we examined the multifractal properties of the VHF time series in the case of the KG EQ, specifically the spectrum of the fractal dimension $D(H)$, as a candidate precursor of the main shock. The results suggest that after the appearance of symmetry breaking the EM time series manifests a reduction of multifractal complexity, displaying a smaller range of local Hurst exponent $H$, while the dominant local Hurst exponent is shifted to higher values (Fig. 5) [3,8]. The observed reduction of multifractality may indicate that the network of fractures becomes less ramified due to anisotropy correlations. Nakaya and Hashimoto [63] have studied the temporal variation of multifractal properties of the seismicity in a region affected by an associated main shock. They find that if a multifractal structure reflects the accumulation of strain energy, then multifractality will decrease prior to the release of a large amount of strain energy accumulated at an asperity.

(ii) In a geometrical sense, both the Hurst exponent and the multifractality specify the strength of the irregularity in

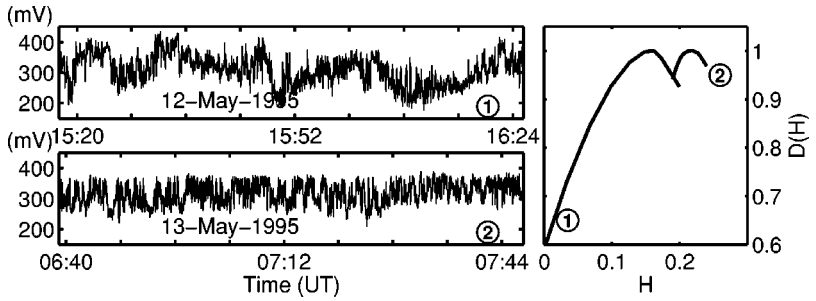


FIG. 5. Two segments of the precursory 41-MHz electromagnetic signal associated with the Kozani-Grevena earthquake recorder on 12 May 1995 (upper row) and 13 May 1995 (lower row). The earthquake occurred on 13 May 1995 at 08:47:12,9 (UTC). In the right part of the figure the corresponding fractal dimensions $D(H)$ are presented [62]. It is clear that as the main shock is approached the EM time series manifests a significant reduction of multifractality.

the EM signal. Ponomarev *et al.* [64] have reported in-phase changes of the temporal and spatial Hurst exponents during sample deformation in laboratory acoustic and EM emission experiments. The fractal dimension $d$ is found from the relation $d=2-H$ for the fractional Brownian motion (fBm) (see section VII) class which, after considering the observed shift of the exponent $H$ to higher values with time, leads to a decrease of fractal dimension as the main event approaches—i.e., a decrease in signal irregularity (see also the next section). On the laboratory scale—e.g., Hirata and Imoto [65]—it is found that the spatial distribution of the hypocenters of the opening cracks ("laboratory EQ's") shows fractal structure. But the fractal dimension significantly decreases with the evolution of the microfracturing process. Recent experiments verify this behavior [66,67]. *These experiments correlate the decrease of the fractal dimension with the concentration of stresses around the family of asperities*.

We think that, taken together, the reduction of multifractality and the decrease of fractal dimension in the precursory VHF EM time series may signal the transition from a sparse cracking distribution to localized cracking within the zone that includes the backbone of strong asperities.

### D. Case of the Athens earthquake

Here we present of the application of the IDCF method and symmetry breaking phenomenon to the 135 MHz preseismic EM signal detected before the Athens EQ [Fig. 1(b)].

In applying the IDCF method, we find at least three time windows which have the properties of a CW. Figure 6 shows one such window, which has a duration of 20 000 sec. The

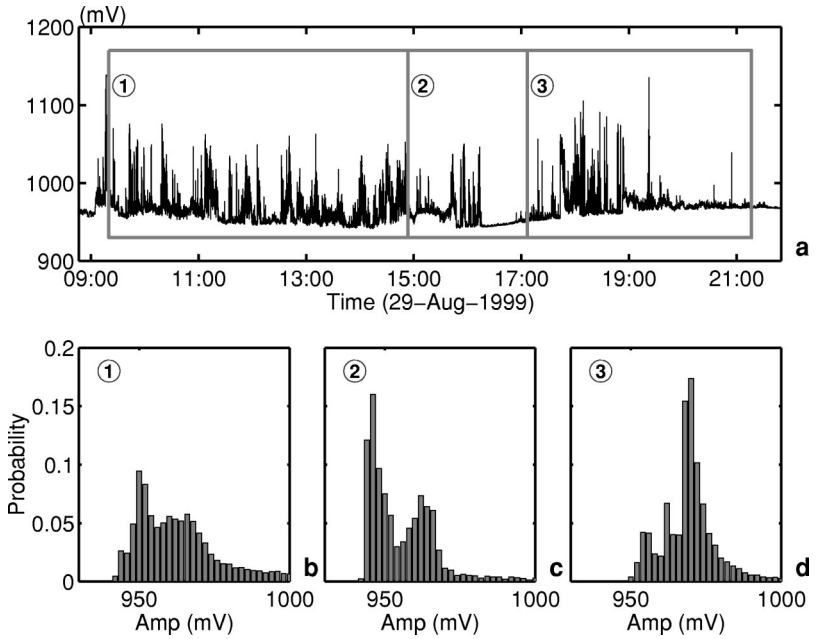


FIG. 6. (a) shows the 135-MHz time series associated with the Athens earthquake. (b)–(d) show the distribution of the amplitude of electromagnetic pulses for four consecutive time intervals marked in (a). The first time interval determines, in terms of the IDCF method [1], the crucial time interval during which the short-range correlations evolve to a long-range critical window; the corresponding distribution (b) might be considered to be a precursor of the impending symmetry breaking readily observable in the subsequent time interval (c). The appearance of the distribution in the (d) may indicate that the symmetry breaking in the underlying fractoelectromagnetic mechanism has been almost completed.

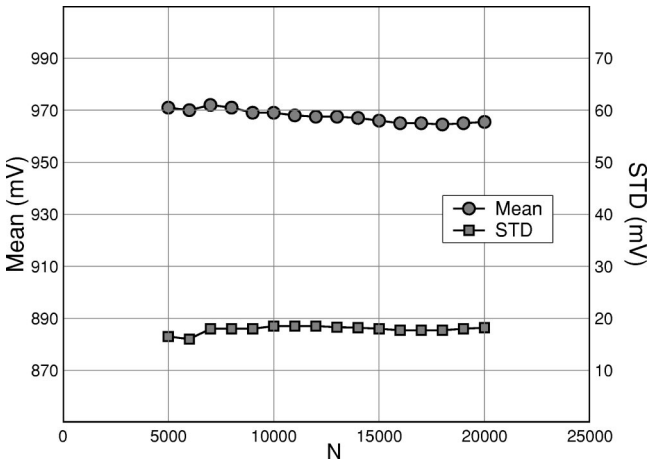


FIG. 7. The cumulative mean value as well as the standard deviation for increasing number of points starting from an initial set of 5000 points. The plot refers to the Athens EQ case.

associated cumulative stationary behavior can be checked by estimating the corresponding mean value (MV) and standard deviation (SDV) of various time intervals in the time series, using a common origin for all intervals. So, starting with a small initial set of data (5000 points), we add each time a number of new data points (1000 points), while estimating the MV and SDV of the corresponding time interval. The results are shown in Fig. 7.

Figure 8 shows the plots of the exponents $p_2$, $p_3$, and Fig. 9 shows the laminar distribution $P(l)$ for the trajectory, where, $p_2$ has its maximum value ($p_2=1.31$) and $p_3$ simultaneously has its minimum value ($p_3=0.0054$). The intermittent dynamics again appears, as in the case of the KG EQ.

Regarding SB, Fig. 6 shows the distribution of the amplitudes of the EM pulses that corresponds to the successive time intervals. We observe a SB effect. Although the temporal evolution of the SB seen in Fig. 6 is similar to that for the KG EQ (Fig. 2), the quality of the associated distributions is not as good. We recall that an outstanding feature of the KG

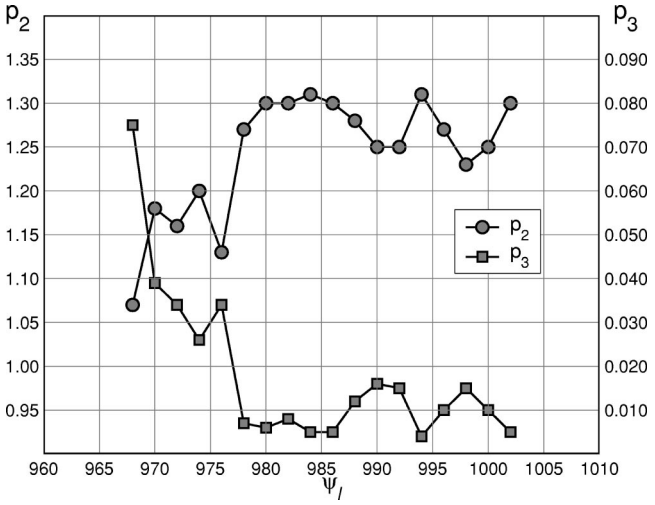


FIG. 8. The exponent $p_2$, $p_3$ versus the end of laminar region $\psi_l$. The analysis refers to the Athens EQ case.

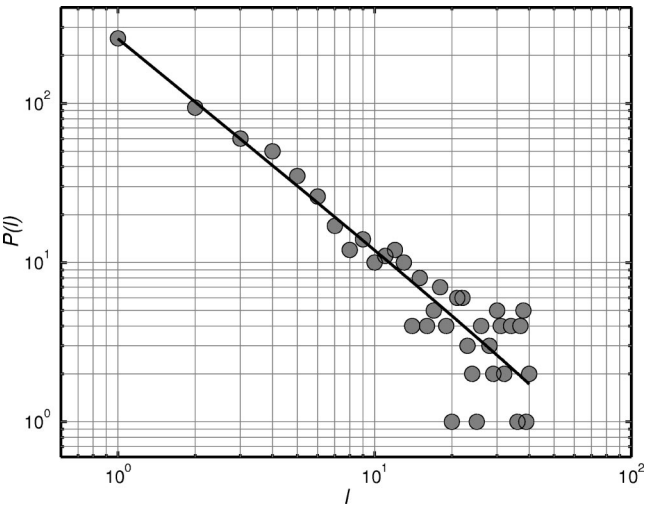


FIG. 9. The distribution $P(l)$ of the laminar intervals $l$. The solid line represent the fitting function $P(l)=p_1 l^{-p_2} e^{-p_3 l}$. The analysis refers to the Athens EQ case.

EQ was the clearly observed extended fault traces [2], while in the case of the Athens EQ the surface part of the crust did not rupture; the energy centroid was 10.3 km for the main fault and 5.4 km for the second one [68]. These observations might explain why the VHF (MHz) part of the preseismic EM anomalies, because of absorption, were weaker in the case of the Athens EQ and thus the hallmarks of the SB evolution were less clear.

## VI. SIGNS INDICATING THAT THE SYSTEM IS DRIVEN OUT OF EQUILIBRIUM

Evidence that the dynamics associated with the critical window is consistent with intermittent dynamics could come out of spectral analysis. There is a theory which refers to the power-law spectrum in intermittent maps of the form (1), known as the $1/f$-noise phenomenon. The spectral density for small frequencies $f$ has the power-law form

$$S(f) \sim f^{-\beta}. \tag{5}$$

Most critical theories have the isothermal critical exponent $\delta > 2 (z > 3)$. To be more specific, mean-field theory has $\delta=3$, gas-liquid (3D Ising) theory has $\delta=5$, and 2D Ising theory has $\delta=15$. For $z>3$ the exponent $\beta$ in the spectral power law (4) is given as [54]

$$\beta = \frac{2z-5}{z-1}. \tag{6}$$

The relation between the exponents $\beta$ and $p_l$ which results from Eqs. (5) and (3) (for $z>3$) is

$$\beta = 5 - 3p_l. \tag{7}$$

From these equations we find that the limits of $p_l$ (for $3<z<\infty$) are $1<p_l<1.5$. So the corresponding limits for the exponent $\beta$ are

$$0.5 < \beta < 2. \quad (8)$$

For completeness we have investigated the $\beta$ exponent limits for theories with $0 < \delta < 2$. In these cases the spectral power laws have the forms [54]

$$2 < z < 3 (1 < \delta < 2): S_f \sim f^{-1/(z-1)},$$

$$\frac{3}{2} < z < 2 (0.5 < \delta < 1): S_f \sim f^{-(2z-3)/(z-1)}.$$

The corresponding limits are $0.5 < \beta < 1$ and $0 < \beta < 1$, respectively.

Taking all the above into account we may say that from the "second-order phase transition" analogy the upper bound for the spectral scaling exponent $\beta$ is $\beta = 2$.

A convenient way to examine transient phenomena is to divide the measurements into time windows and analyze these windows. If this analysis yields different results for some precursory time intervals, then a transient behavior can be extracted. Recently [3] we calculated the scaling exponent $\beta$ associated with successive intervals of 1024 measurements each and studied the time evolution of this parameter in the VHF EM precursory time series detected prior to the KG EQ. The data were sampled at 1 Hz. We observed a systematic increase of the $\beta$ exponent with time, but within the range (1, 2) and therefore within the upper bound given above. We interpret the systematic increase as indicating that the system was gradually being driven out of equilibrium. What happens when $\beta$ exceeds 2? In the next section we attempt to shed more light on the physical significance of the upper limit $\beta = 2$ by considering the fracture process.

## VII. STUDY OF THE PRESEISMIC EM RADIATION IN TERMS OF HETEROGENEITY

Two classes of signal have been widely used to model stochastic fractal time series [69]: fractional Gaussian noise (fGn) and fractional Brownian motion (fBm). These are, respectively, generalizations of white Gaussian noise and Brownian motion. A formal mathematical definition of continuous fBm was first offered by Mandelbrot and Ness [70]. For the case of the fBm model the scaling exponent $\beta$ lies between 1 and 3, while the regime of fGn [69] is indicated by $\beta$ values from $-1$ to 1. The $\beta$ values in the VHF EM prefracture time series are distributed in the region from 1 to 2. This means that the seismogenic EM activity follows the fBm model.

The exponent $\beta$ is related to another exponent, the Hurst exponent $H$, by the formula [71]

$$\beta = 2H + 1 \quad (9)$$

for the fBm model [69,70].

$H$ can lie anywhere in the range $0 < H < 1$ and characterizes the persistent and antipersistent properties of the signal according to the following scheme. (i) The range $0.5 < H < 1$ $(2 < \beta < 3)$ suggests persistence of the signal (superdiffusion); i.e., if the amplitude of EM fluctuations increases in a time interval, it is likely to continue increasing in the interval immediately following. (ii) The range $0 < H < 0.5$ $(1 < \beta < 2)$ suggests antipersistency; i.e., if the EM fluctuations increase in a period, they are likely to continue decreasing in the interval immediately following and vice versa. (iii) $H = 0.5$ $(\beta = 2)$ indicates no correlation between successive increments.

The particular value $\beta = 2$ (or $H = 0.5$) implies a transition from antipersistent to persistent behavior during the evolution of the prefracture EM activity. In the previous section we concluded that the IDCF method is not applicable if the associated $\beta$ value exceeds the bound $\beta = 2$ (or $H = 0.5$). We attempt to understand the physics behind this.

The interplay between the heterogeneities and the stress field could be responsible for the observed pattern of the precursory EM time series under study. Indeed, in natural rock at large length scales there are long-range anticorrelations, in the sense that a high value of a rock property (e.g., threshold for breaking) is followed by a low value and vice versa (Refs. [72,73], and references therein). The antipersistent character of the EM time series may reflect the fact that in heterogeneous media, volumes with a low threshold for breaking alternate with much stronger volumes. Crack growth in a heterogeneous medium continues until a much stronger region is encountered. When this happens, crack growth stops while another crack nucleates in a weaker region and so on. An observed decrease of antipersistent behavior may be an indication that the heterogeneity in the prefocal area is becoming less anticorrelated with time.

Antipersistent behavior implies a set of fluctuations tending to induce a stability within the system—i.e., a nonlinear negative feedback, which "kicks" the opening cracks away from extremes. An observed systematic increase of the $H$ exponent in the range from 0 to 0.5 indicates that the fluctuations are becoming less anti correlated with time. This implies that the non linear negative feedback mechanism is gradually losing its ability to "kick" the system away from extremes. The system gradually is driven out of equilibrium.

Consequently, heterogeneity could account for the appearance of a stationary-like behavior in the antipersistent part of the prefracture EM time series and thus enable the fracture in highly heterogeneous systems to be described via an analogy with thermal continuous phase transition.

In the case of a homogenous rock, the stress is enhanced at its tip and therefore the next microcrack almost surely develops at the tip. Thus, one expects to see long-range positive correlations—i.e., persistent behavior $(0.5 < H < 1)$ in the associated EM emission. Indeed, the abrupt emergence of strong VLF emission in the tail of the precursory EM radiation, showing persistent behavior, may be regarded as a fingerprint of the local dynamic fracture of nearly homogeneous strong asperities in the focal zone (see Sec. VIII).

In summary, the bound $H = 0.5$ may signal the transition from a heterogeneous to a homogeneous regime during the EQ preparation process. This situation would also explain why fracture in a homogeneous medium could not be described by an analogy with thermal continuous phase transition.

Despite the many efforts and successes that have been recently achieved, the issue of whether rupture exhibits properties analogous to either a first-order or a second-order ther-

modynamic phase transition remains under discussion. Our results verify that fracture in heterogeneous systems with long-range antipersistent interactions can be described as analogous to a phase transition of second order. In addition, our results suggest that fracture in homogeneous systems with long-range persistent interactions is a nonequilibrium process. In fracture mechanics, the democratic fiber bundle model (DFBM) exhibits an interesting transition as a function of the amplitude of the disorder. There exists a tricritical transition [15] from a Griffith-type abrupt rupture (i.e., "first-order") regime, where rupture occurs without significant precursors, to a progressive damage (i.e., "second-order") regime as the disorder increases. We argue that the observed features in the precursory EM emission are in agreement with this scheme. The emergence of persistent dynamics seems to signal the transformation of the critical regime to abrupt "first-order" behavior.

## VIII. EVIDENCE INDICATING THE FRACTURE OF ASPERITIES

A backbone of asperities in a heterogeneous medium behaves as a stress concentrator. It acts not only as a rupture arrestor but also as a rupture initiator. The question arises as to *whether precursory EM phenomena can also reveal the fracture of the high-strength homogeneous asperities if and when the local stress exceeds their fracture stress*.

We discuss in this section the hypothesis that the *abrupt* strong impulsive kilohertz EM activity in the tail of the precursory EM activity seen in Fig. 1 signals the fracture of asperities in the focal area.

First we focus on the case of the KG EQ. We recall that at 3 kHz and 10 kHz very strong multipeaked signals with sharp onsets and decays emerged in the tail of the megahertz activity. The power spectrum of the VLF activity shows a decreasing power-law behavior $S(f) \sim f^{-\beta}$ with two different branches, one at lower $(r=0.92, \beta=1.04)$ and another at higher frequencies $(r=0.99, \beta=2.91)$ [3]. The power law at higher frequencies may reflect the dynamics within the bursts, while the one at lower frequencies may indicate the correlation between the bursts [74]. This would indicate that the EM fluctuations within the bursts, and thus the microfractures within the asperities, show very strong persistent behavior ($H=0.96$), as would be expected in a homogeneous medium. The multifractal analysis of this signal at higher frequencies also reveals the underlying persistent dynamics: the local Hurst exponents are centered at $H \sim 0.85$ [3].

Now consider the Athens EQ. The precursory EM phenomenon ends in two very strong impulsive kilohertz signals [Figs. 1(b) and 10], which also show strong persistent behavior (Fig. 10) [3,8].

We mentioned in Sec. III that the IDCF method suggests that scaling critical theory cannot be valid in the persistent regime. Indeed, the meaning which we have attributed to the critical time window does not encourage the presence of such a window in the persistent VLF activity. Nevertheless, we systematically searched for the presence of VLF time window which had the characteristics of a critical window. The result of this search was negative. This is further indication that the associated phase of the EQ generation is a nonequilibrium process without any footprint of an equilibrium phase transition.

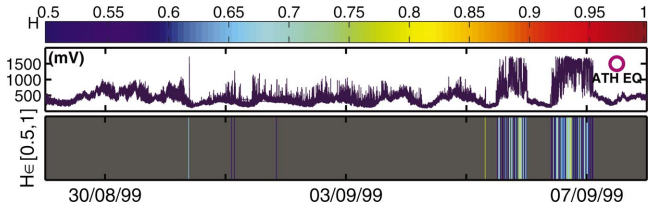


FIG. 10. Decomposition of the precursory 10-kHz EM time series associated with the Athens EQ into subsets, each characterized by a different Hurst exponent *H*. The Hurst exponent is color coded by the rainbow, so that each subset has a different color. We observe that persistent behavior is emerged within the two strong impulsive electromagnetic bursts in the tail of the precursory radiation.

Laboratory studies support the hypothesis that the persistent part of the EM precursory emission may correspond to the nucleation phase of the EQ preparation process. We mention here some relevant observations.

Experiments in terms of acoustic emission reveal a significant shift from MHz to kHz, just before global failure (97%–100% of the failure strength) [2]. (Recall that the strong persistent VLF emission emerges in the tail of the EM activity.) And recent experiments in terms of acoustic and EM emission show that the main rupture occurs after the appearance of strong persistent behavior [64] in the corresponding time series.

Laboratory studies under well-controlled conditions—i.e., using well-prepared samples containing well-known asperities—should be useful for understanding the physics of asperities. Recently Lei *et al.* [66,67] have studied how an individual asperity fractures, how coupled asperities fracture, and also the role of asperities in fault nucleation and as potential precursors prior to dynamic rupture. These observations reveal a strong similarity between the fracture of asperities in laboratory-scale experiments and tectonic-scale events. More precisely, they suggest the following. (i) Intense microcracking may occur in a strong asperity when the local stress exceeds the fracture stress of the asperity. This feature is in agreement with our results. (ii) The self-excitation strength, which expresses the influence of excitation of an event on succeeding events or, equivalently, the degree of positive feedback in the dynamics, reaches a maximum of $\sim 1$ during the nucleation phase of the fault. Recall that the *H* exponent also approaches its maximum value of 1 in the tail of the precursory EM radiation. (iii) The fractal dimension decreases from $\sim 2.2$ in the prenucleation phase to 1.0–1.4 during asperity fracture. Recall that the fractal dimension also drops to about 1 in the tail of the precursory EM time series detected prior to the Athens and KG EQ's.

Although there remain significant problems in extrapolating laboratory results to field conditions, the above experimental findings may indicate that the emergence of strong positive correlations reflect the faulting nucleation phase of EQ preparation—namely, the fracture of the sequence of asperities in the focal area.

Geophysical observations associated with the Athens and KG EQ's further support our hypothesis. First, the two strong

VLF EM bursts before the Athens EQ show persistent behavior, as mentioned earlier (Fig. 10). The first EM signal contains approximately 20% of the total EM energy received and the second contains the remaining 80% [4]. On the other hand, the fault modeling of the Athens EQ, based on information obtained by both radar interferometry and seismological measurements [4,68], predicts two faults. The main fault segment is responsible for 80% of the total energy released, with the secondary fault releasing the remaining 20% [4]. This is a strong correlation between results in the EM and energy domains. Second, a sequence of five foreshocks observed before the KG EQ, clustered within 2 km of one another about 5–10 km from the main shock epicenter, occurred after the cessation of the EM anomalies [75]. The observation of foreshocks is the most convincing evidence for a nucleation stage before major earthquakes. The strong VLF activity, embedded in a long-duration EM quiescence in this frequency band [2], ceased almost 1 h before the EQ. This unusual foreshock activity may be regarded as a fingerprint of the local dynamic rupture of asperities.

### VLF EM emission and the self-affine asperity model for earthquakes

Recently, a self-affine asperity model (SAM) for EQ's has been introduced [76,77]. This model mimics the friction between moving faults by means of two fractional Brownian profiles that slide over one another. The distribution of areas of the broken asperities follows the power law $P(A_{asp}) \sim A_{asp}^{-\zeta}$, with an exponent $\zeta$ which may be related analytically to the roughness of the fault. In this scheme, an EQ occurs when there is an intersection between the two profiles representing the two fault faces. The energy released is assumed proportional to the overlap. If we accept that the released EM energy is also proportional to the degree of overlap, which means that it is proportional to the number broken interatomic bonds (see Sec. II), a power-law distribution of the amplitudes in the preseismic EM series is expected. Recall from Sec. II that our analysis reveals that the sequence of precursory VLF EM pulses associated with the Athens EQ follows the power law-distribution $N(>A) \sim A^{-0.62}$ [1]. This observed power-law behavior may stem from the fractal geometry of the asperities and is well connected with the intermittency that is observed.

## IX. ELECTROMAGNETIC QUIESCENCE JUST BEFORE THE MAIN SHOCK

An interesting characteristic of preseismic EM emissions is the appearance of quiescence in all frequency bands during the last few hours before the main shock [24,78–81]. This prefracture EM "quiescent" period has also been observed in laboratory-scale experiments [20,24,82].

Laboratories studies of acoustic and EM emissions indicate that the acoustic signals are recorded directly before and during the fragmentation of the specimen, while kilohertz EM emission precedes this stage [24,34]. This behavior corresponds very well to our field observation for the KG EQ: The recorded kilohertz EM emission ceased approximately 60 min prior to the main shock; after that, several foreshocks clustered a few kilometers around the eventual epicenter [75] emerged during the last ~30 min min before the EQ.

Laboratory experiments indicate that the efficiency of generating EM emission is higher in tensile cracks than in shear cracks [20]. We view the EM phenomena discussed here to be a result of electrification of the "fresh" crack surface. In this picture it is reasonable to expect EM quiescence just before the main shock, because the latter is considered to be a result of shear faulting, which may not be very efficient for creation of a fresh surface [20].

In a recent paper [3], we suggested that the EM quiescence just before the main shock (i.e., global failure) may signal the expected catastrophic decrease in the elastic modulus $M$ [83–85]. Kachanov [84] has presented several models that predict a reduction of the effective modulus of an elastic solid due to multiple distributed cracks. The sudden drop of the elastic modulus could be due to an abrupt decrease in the amount of energy that can be released during crack nucleation close to the mechanical percolation threshold. Thus the amplitude of EM emissions should decrease before final rupture [85].

In summary, the appearance of EM quiescence would seem to be a further indication of a high probability for a global instability ensuing within a few hours of the quiescent period.

## X. CONCLUSIONS

In the present work, in which we view earthquakes as large-scale fracture phenomena, we have attempted to put forward physically meaningful arguments to support (i) a way of quantifying the time to global failure and (ii) the identification of distinguishing features beyond which the evolution towards global failure becomes irreversible. Our method is based on monitoring the microfractures, which occur in the prefocal area before the final breakup, by recording their VLF (kHz)–VHF (MHz) EM emissions.

The focal area has been modeled by (i) a backbone of strong and large asperities that sustains the system and (ii) a strongly heterogeneous medium that surrounds the family of strong asperities.

The analysis in terms of the method of intermittent dynamics of critical fluctuations suggests that the initial VHF (MHz) part of the prefracture EM emission, which has antipersistent behavior, is triggered by microfractures in the highly disordered heterogeneous component and could be described in analogy with a thermal continuous phase transition. Considerations of symmetry breaking in the IDCF method reveal that the system is gradually driven out of equilibrium. This evidence motivated us to estimate the time beyond which the process generating the preseismic EM emission could continue only as a nonequilibrium instability.

Our results suggest that nonequilibrium is to be viewed as a state of matter exhibiting positive long-range correlations. Dense persistent microcracking and, thus, dense persistent EM radiation may then occur in the strong asperities if and when the local stress exceeds their fracture stress. The abrupt emergence of strong VLF emission in the tail of the precur-

sory EM radiation, showing persistent behavior, may be regarded as a fingerprint of the local dynamic fracture of asperities in the focal zone—namely, faulting nucleation. This is supported by information obtained from radar interferometry and seismological observations. In addition, laboratory studies indicate the emergence of dense VLF acoustic emission in the tail of prefracture VHF acoustic emission during the final prefailure stage, as well as the emergence of persistent properties during the fracture of asperities.

In terms of the underlying physics, the appearance of persistent properties may indicate that the process is being driven as a nonequilibrium instability, thus acquiring a self-regulating character and to a great degree the property of irreversibility. This latter is one of the important components of prediction reliability.

A catastrophic decrease in the elastic modulus just before the final rupture is expected. The appearance of an EM gap in all the frequency bands might be considered as a hallmark that the expected decrease in the elastic modulus has occurred. So the existence of a quiescent period may constitute the last clue that a significant seismic event is forthcoming with a considerable probability.

On the basis of our study, drawing on both field observations and laboratory experiments on rock fracture, we make the following suggestions concerning the initial and final times for the critical last stages of the EQ preparation process. The initial point corresponds to the occurrence of distinguishing features beyond which the evolution towards global failure becomes essentially irreversible. The final point corresponds to the onset of a quiescent period when all precursory EM actively ceases. While this analysis may point to a possible way of estimating the time to global failure, at least for in-land seismic events which are both strong and shallow, further work in this direction is certainly needed.

## ACKNOWLEDGMENTS

We would like to thank G. Bambakidis for a critical reading of the manuscript. This work was supported by the European Union (epeaek-Pythagoras No. 70/3/7357).

[1] P. Kapiris, G. Balasis, J. Kopanas, G. Antonopoulos, A. Peratzakis, and K. Eftaxias, Nonlinear Processes Geophys. **11**, 137 (2004).
[2] K. Eftaxias, P. Kapiris, E. Dologlou, J. Kopanas, N. Bogris, G. Antonopoulos, A. Peratzakis, and V. Hadjicontis, Geophys. Res. Lett. **29**, 69/1 (2002).
[3] P. Kapiris, K. Eftaxias, and T. Chelidze, Phys. Rev. Lett. **92**, 065702 (2004).
[4] K. Eftaxias, P. Kapiris, J. Polygiannakis, N. Bogris, J. Kopanas, G. Antonopoulos, A. Peratzakis, and V. Hadjicontis, Geophys. Res. Lett. **28**, 3321 (2001).
[5] K. Eftaxias, P. Kapiris, J. Polygiannakis, A. Peratzakis, J. Kopanas, and G. Antonopoulos, Nat. Hazards Earth Syst. Sci. **3**, 217 (2003).
[6] P. Kapiris, J. Polygiannakis, K. Nomicos, and K. Eftaxias, Earth, Planets Space **54**, 1237 (2002).
[7] P. Kapiris, K. Eftaxias, K. Nomikos, J. Polygiannakis, E. Dologlou, G. Balasis, N. Bogris, A. Peratzakis, and V. Hadjicontis, Nonlinear Processes Geophys. **10**, 1 (2003).
[8] K. Eftaxias, P. Frangos, P. Kapiris, J. Polygiannakis, J. Kopanas, A. Peratzakis, P. Skountzos, and D. Jaggard, Fractals **12**, 243 (2004).
[9] Y. Contoyiannis, F. Diakonos, P. Kapiris, and K. Eftaxias, Phys. Chem. Earth **29**, 397 (2004).
[10] Y. Contoyiannis, F. Diakonos, and A. Malakis, Phys. Rev. Lett. **89**, 035701 (2002).
[11] Y. Contoyiannis and F. Diakonos, Phys. Lett. A **268**, 286 (2000).
[12] H. Herrmann and S. Roux, *Statistical Models for Fracture of Disordered Media* (North-Holland, Amsterdam, 1990).
[13] C. Vanneste and D. Sornette, J. Phys. I **2**, 1621 (1992).
[14] L. Lamaignere, F. Carmona, and D. Sornette, Phys. Rev. Lett. **77**, 2738 (1996).
[15] J. Andersen, D. Sornette, and K. Leung, Phys. Rev. Lett. **78**, 2140 (1997).
[16] D. Sornette, *Critical Phenomena in Natural Sciences* (Springer, Berlin, 2000).
[17] V. Nitsan, Geophys. Res. Lett. **4**, 333 (1977).
[18] J. Warwick, C. Stoker, and T. Meyer, J. Geophys. Res. **87**, 2851 (1982).
[19] T. Ogawa, K. Oike, and T. Miura, J. Geophys. Res. **90**, 6245 (1985).
[20] I. Yamada, K. Masuda, and H. Mizutani, Phys. Earth Planet. Inter. **57**, 157 (1989).
[21] V. Petrenko and O. Gluschenkov, J. Geophys. Res., [Solid Earth] **101**, 11541 (1996).
[22] V. Frid, A. Rabinovitch, and D. Bahat, Philos. Mag. Lett. **79**, 79 (1999).
[23] C. Mavromatou and V. Hadjicontis, in *Earthquake Thermodynamics and Phase Transformations in the Earth's Interior*, edited by R. Teisseyre and E. Majewski (Academic Press, San Diego, 2001), pp. 501–517.
[24] V. Morgounov, Ann. Geofis. **44**, 369 (2001).
[25] A. Rabinovitch, V. Frid, and D. Bahat, Phys. Rev. E **65**, 011401 (2001).
[26] D. Bahat, V. Frid, A. Rabinovitch, and V. Palchik, Int. J. Fract. **116**, 179 (2002).
[27] C. Mavromatou, V. Hadjicontis, D. Ninos, D. Mastrogiannis, E. Hadjicontis, and K. Eftaxias, Phys. Chem. Earth **29**, 353 (2004).
[28] M. Hayakawa and Y. Fujinawa, *Electromagnetic Phenomena Related to Earthquake Prediction* (Terrapub, Tokyo, 1994).
[29] M. Hayakawa, *Atmospheric and Ionospheric Electromagnetic Phenomena Associated with Earthquakes* (Terrapub, Tokyo, 1999).
[30] M. Hayakawa and O. Molchanov, *Seismo Electromagnetics* (Terrapub, Tokyo, 2002).
[31] Seismo Electromagnetics and Related Phenomena, edited by M. Hayakawa, O. Molchanov, P. Biagi, and F. Vallianatos, special issue of Phys. Chem. Earth **29**, 287 (2004)].

[32] T. Lokajvcek and J. Sikula, Prog. Acoust. Emission VIII 311 (1996).
[33] A. Rabinovitch, V. Frid, D. Bahat, and J. Goldbaum, Int. J. Rock Mech. Min. Sci. **37**, 1149 (2000).
[34] P. Koktavy, J. Pavelka, and J. Sikula, Meas. Sci. Technol. **15**, 973 (2004).
[35] A. Rabinovitch, V. Frid, and D. Bahat, Philos. Mag. Lett. **77**, 289 (1998).
[36] S. Langford, J. Dickinson, and L. Jensen, J. Appl. Phys. **62**, 1437 (1987).
[37] G. Cress, B. Brady, and G. Rowell, Geophys. Res. Lett. **14**, 331 (1987).
[38] Y. Enomoto, T. Shimamoto, A. Tsutsumi, and H. Hashimoto, in *Electromagnetic Phenomena Related to Earthquake Prediction*, edited by M. Hayakawa and Y. Fujinawa (Terrapub, Tokyo, 1994), pp. 253–259.
[39] J. Wolibrandt, U. Bruckner, and E. LInke, Phys. Status Solidi A **77**, 545 (1983).
[40] J. Dickinson, S. Langford, L. Jensen, G. McVay, J. Kelso, and C. Pantano, J. Vac. Sci. Technol. A **6**, 1084 (1988).
[41] A. C. Gonzalez and C. G. Pantano, Appl. Phys. Lett. **57**, 246 (1990).
[42] T. Miura and K. Nakayama, J. Appl. Phys. **88**, 5444 (2000).
[43] M. Miroshnichenko and V. Kuksenko, Sov. Phys. Solid State **22**, 895 (1980).
[44] N. Khatiashvili, Phys. Solid Earth 20, 656 (1984).
[45] S. O'Keefe and D. Thiel, Phys. Earth Planet. Inter. **89**, 127 (1995).
[46] M. Marder and J. Fineberg, Phys. Today **49**(9), 24 (1996).
[47] E. Sharon and J. Fineberg, Phys. Rev. B **54**, 7128 (1996).
[48] E. Sharon and J. Fineberg, Nature (London) **397**, 333 (1999).
[49] E. Sharon, S. Gross, and J. Fineberg, Phys. Rev. Lett. **74**, 5096 (1995).
[50] A. Sornette and D. Sornette, Tectonophysics **179**, 327 (1990).
[51] D. Jaggard, in *Recent Advances in Electromagnetic Theory*, edited by H. Kritikos and D. Jaggard (Springer-Verlag, New York, 1990), pp. 183–224.
[52] D. L. Jaggard, A. D. Jaggard, and P. Frangos, in *Frontiers in Electrodynamics*, edited by D. Werner and R. Mittra (IEEE Press, New York, 2000), pp. 1–47.
[53] Y. Contoyiannis, F. Diakonos, C. Papaefthimiou, and G. Theophilidis, Phys. Rev. Lett. **93**, 098101 (2004).
[54] H. Schuster, *Deterministic Chaos* (VCH, Weinheim, 1998).
[55] Y. Moreno, J. Gomez, and A. Pacheco, Phys. Rev. Lett. **85**, 2865 (2000).
[56] H. Jensen, *Self-Organized Criticality* (Cambridge University Press, Cambridge, England, 1998).
[57] G. Caldarelli, C. Castellano, and A. Petri, Physica A **270**, 15 (1999).
[58] T. Harris, *The Theory of Branching Processes* (Springer-Verlag, Berlin, 1963).
[59] D. Sornette and J. Andersen, Eur. Phys. J. B **1**, 353 (1998).
[60] J. Kolesnikov and T. Chelidze, J. Phys. A **18**, 273 (1985).
[61] T. Chelidze, T. Reuschle, and Y. Gueguen, J. Phys.: Condens. Matter **6**, 1857 (1994).
[62] P. Ivanov, L. Amaral, A. Goldberger, S. Havlin, M. Rosenblum, Z. Struzik, and H. Stanley, Nature (London) **399**, 461 (1999).
[63] S. Nakaya and T. Hashimoto, Geophys. Res. Lett. **29**, 133 (2002).
[64] A. Ponomarev, A. Zavyalov, V. Smirnov, and D. Lockner, Tectonophysics **277**, 57 (1997).
[65] T. Hirata and M. Imoto, Geophys. J. Int. **107**, 155 (1991).
[66] X. Lei, O. Nishizawa, K. Kusunose, A. Cho, T. Satoh, and O. Nishizawa, Tectonophysics **348**, 329 (2000).
[67] X. Lei, K. Masuda, O. Nishizawa, L. Jouniaux, L. Liu, W. Ma, T. Satoh, and K. Kusunose, J. Struct. Geol. **26**, 247 (2004).
[68] C. Kontoes, P. Elias, O. Sycioti, P. Briole, D. Remy, M. Sachpazi, G. Veis, and I. Kotsis, Geophys. Res. Lett. **27**, 3989 (2000).
[69] C. Heneghan and G. McDarby, Phys. Rev. E **62**, 6103 (2000).
[70] B. Mandelbrot and J. Ness, SIAM Rev. **10**, 422 (1968).
[71] D. Turcotte, *Fractals and Chaos in Geology and Geophysics* (Cambridge University Press, Cambridge, England, 1992).
[72] M. Sahimi, Rev. Mod. Phys. **65**, 1393 (1993).
[73] M. Sahimi and S. Arbabi, Phys. Rev. Lett. **77**, 3689 (1996).
[74] M. Kuntz and P. Sethna, Phys. Rev. B **62**, 11 699 (2000).
[75] P. Bernard, P. Pinettes, P. Hadjidimitriou, E. Scordilis, G. Veis, and P. Milas, Geophys. J. Int. **131**, 467 (1997).
[76] V. D. Rubeis, R. Hallgass, V. Loreto, G. Paladin, L. Pietronero, and P. Tosi, Phys. Rev. Lett. **76**, 2599 (1996).
[77] R. Hallgass, V. Loreto, O. Mazzella, G. Paladin, and L. Pietronero, Phys. Rev. E **56**, 1346 (1997).
[78] V. Morgounov, T. Ondoh, and S. Nagai, in *Electromagnetic Phenomena Related to Earthquake Prediction*, edited by M. Hayakawa and Y. Fujinawa (Terrapub, Tokyo, 1994), pp. 409–428.
[79] S. Qian, J. Yian, H. Cao, S. Shi, Z. Lu, J. Li, and K. Ren, in Electromagnetic Phenomena Related to Earthquake Prediction, edited by M. Hayakawa and Y. Fujinawa (Terrapub, Tokyo, 1994), pp. 205–211.
[80] T. Nagao, Y. Orihara, T. Yamaguchi, T. Takahashi, K. Hattori, Y. Noda, and K. Sayanagi, Geophys. Res. Lett. **27**, 1535 (2000).
[81] K. Eftaxias, J. Kopanas, N. Bogris, P. Kapiris, G. Antonopoulos, and P. Varotsos, Proc. Jpn. Acad., Ser. B: Phys. Biol. Sci. **76**, 45 (2000).
[82] D. Barber and P. Meredith, *Deformation Processes in Minerals, Ceramics and Rocks* (Unwin Human, London, 1990).
[83] M. Sahimi and J. Goddard, Phys. Rev. B **33**, 7848 (1986).
[84] M. Kachanov, Appl. Mech. Rev. **45**, 304 (1992).
[85] T. Chelidze, Terra Nova **5**, 421 (1993).